Annu. Rev. Phys. Chem. 2018.69:273-298. Downloaded from www.annualreviews.org
Access provided by Cambridge University on 04/22/18. For personal use only.

ANNUAL REVIEWS

Annual Review of Physical Chemistry

Chemical Kinetics for Bridging Molecular Mechanisms and Macroscopic Measurements of Amyloid Fibril Formation

Thomas C.T. Michaels,[1,2] Anđela Šarić,[3] Johnny Habchi,[1] Sean Chia,[1] Georg Meisl,[1] Michele Vendruscolo,[1] Christopher M. Dobson,[1] and Tuomas P.J. Knowles[1,4]

[1]Centre for Misfolding Diseases, Department of Chemistry, University of Cambridge, Cambridge CB2 1EW, United Kingdom; email: tpjk2@cam.ac.uk

[2]Paulson School of Engineering and Applied Sciences, Harvard University, Cambridge, Massachusetts 02138, USA

[3]Department of Physics and Astronomy, and Institute for the Physics of Living Systems, University College London, London WC1E 6BT, United Kingdom

[4]Cavendish Laboratory, Department of Physics, University of Cambridge, Cambridge CB3 1HE, United Kingdom; email: mv245@cam.ac.uk, cmd44@cam.ac.uk

ANNUAL REVIEWS **Further**

Click here to view this article's online features:

- Download figures as PPT slides
- Navigate linked references
- Download citations
- Explore related articles
- Search keywords

Annu. Rev. Phys. Chem. 2018. 69:273–98

First published as a Review in Advance on February 28, 2018

The *Annual Review of Physical Chemistry* is online at physchem.annualreviews.org

https://doi.org/10.1146/annurev-physchem-050317-021322

Copyright © 2018 by Annual Reviews.
All rights reserved

Keywords

protein misfolding, protein aggregation, Alzheimer's disease, neurodegenerative diseases, self-assembly, rate law, master equation, reaction order, scaling exponent, global fit, secondary nucleation, oligomers, inhibition, drug discovery, computer simulations, coarse-grained simulations

Abstract

Understanding how normally soluble peptides and proteins aggregate to form amyloid fibrils is central to many areas of modern biomolecular science, ranging from the development of functional biomaterials to the design of rational therapeutic strategies against increasingly prevalent medical conditions such as Alzheimer's and Parkinson's diseases. As such, there is a great need to develop models to mechanistically describe how amyloid fibrils are formed from precursor peptides and proteins. Here we review and discuss

how ideas and concepts from chemical reaction kinetics can help to achieve this objective. In particular, we show how a combination of theory, experiments, and computer simulations, based on chemical kinetics, provides a general formalism for uncovering, at the molecular level, the mechanistic steps that underlie the phenomenon of amyloid fibril formation.

Annu. Rev. Phys. Chem. 2018.69:273-298. Downloaded from www.annualreviews.org
Access provided by Cambridge University on 04/22/18. For personal use only.

1. INTRODUCTION

1.1. What Is Amyloid Fibril Formation?

The aggregation of proteins and peptides into amyloid fibrils is a ubiquitous example of linear, molecular self-assembly. A large number of peptides and proteins with very different sequences and structural folds can aggregate into amyloid fibrils that possess a common characteristic structure rich in β-sheets (**Figure 1**; see also the sidebar titled What Are Amyloid Fibrils?) (1, 2). These observations suggest that general physical principles are likely to be particularly effective for describing this and other related self-assembly phenomena. A central problem in this area is how to interpret macroscopic physical observables determined in experiments in terms of the fundamental microscopic mechanisms that give rise to the overall aggregation behavior. Bridging this gap from microscopic to macroscopic scales requires a detailed understanding of the fundamental processes of amyloid formation at all intermediate length and timescales. Methods rooted in the physical sciences and historically applied to analyze the dynamics of other complex systems have emerged as a key component in addressing this challenge, enabling us to develop an increasingly detailed molecular picture of amyloid fibril formation. These advances hold great promise for biomolecular science, and in this review we discuss how the introduction of concepts from chemical reaction kinetics has generated fundamental advances in our understanding of amyloid aggregation. Broadly, this involves clarifying core questions, such as: Why do proteins or peptides self-assemble into amyloid fibrils? Through which molecular mechanisms do they do so? Which of these molecular steps cause toxicity or involve toxic species? How can we interfere with amyloid

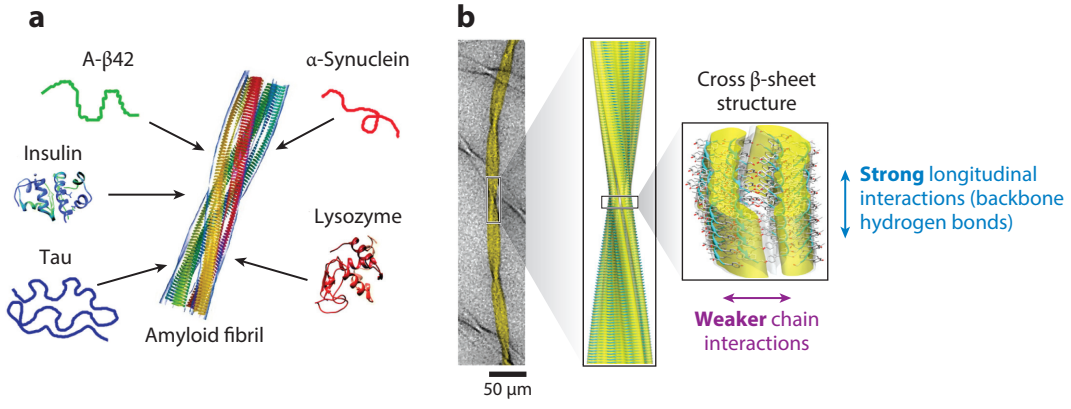

Figure 1

(*a*) Generic nature of amyloid fibril formation. (*b*) Hierarchical structure of one polymorph of the amyloid fibrils formed by an 11-residue fragment of transthyretin as determined by cryo-electron microscopy imaging and solid-state nuclear magnetic resonance spectroscopy (3). In this example, the mature amyloid fibril is composed of three filaments twisted around one another, and each one of these filaments is composed of two cross β-sheet protofilaments. Panel *a* adapted from References 4, 5. Panel *b* adapted from Reference 3.

WHAT ARE AMYLOID FIBRILS?

There are two main definitions of amyloid fibrils. According to the original medical definition, amyloids are extracellular protein deposits that can be detected through a characteristic apple-green fluorescence when stained with Congo red and visualized under polarized light. According to the more recent biophysical definition (6), amyloid fibrils are an important class of filamentous structures that result from the assembly of normally monomeric proteins or peptides and that feature a characteristic core structure rich in β-sheets. In this article, we adopt the biophysical definition, as it is more general. Like many other biological and biomimetic materials, amyloid fibrils possess a hierarchical structure across different length scales, from the macroscopic scale down to the molecular and atomic scales. In particular, structural studies have shown that amyloid fibrils typically consist of a number of filaments wound around one another. Each of these filaments is composed of cross-β protofilaments held together by specific side-chain interactions, with cross-β protofilaments consisting, in turn, of a supramolecular stack of β-sheets composed of β-strands aligned perpendicularly to the long fibril axis and connected laterally through stronger backbone hydrogen bonds (1, 7–11). At the highest level of hierarchy, mature amyloid fibrils can assemble with other fibrils to form amyloid plaques and films, which can be observed as deposits in the brains of Alzheimer's disease patients in the case of the amyloid-β peptide. Typically, a mature amyloid fibril can extend up to 10 μm in length and has cross-sectional dimensions in the range 2–20 nm (12, 13). Monomer–monomer interactions in amyloid fibrils involve directional hydrogen bonding as well as other possible intermolecular interactions, such as hydrophobic, van der Waals, and screened electrostatic interactions, and typically extend over spatial scales ranging from a few angstroms to several nanometers. The dense network of backbone hydrogen bonds that characterizes the cross-β structure of amyloid fibrils grants them characteristic materials properties, such as high bending rigidity (14). Moreover, the large number of strong hydrogen-bonding interactions between the constituent molecules renders amyloid fibrils energetically favorable structures (14). The thermodynamic stability of the amyloid state could be the reason why so many different and apparently unrelated proteins and peptides share the ability to form amyloid fibrils (1, 2, 15).

Annu. Rev. Phys. Chem. 2018.69:273-298. Downloaded from www.annualreviews.org
Access provided by Cambridge University on 04/22/18. For personal use only.

aggregation to prevent or suppress its associated toxicity for therapeutic purposes? With these questions to guide us, this review is structured as follows. First, we review some relevant concepts and notions from chemical kinetics and discuss their implications in the context of studying reaction mechanisms for amyloid aggregation kinetics. We then provide an overview of recent advances in the use of coarse-grained simulations to understand amyloid fibril formation. Finally, we discuss applications of chemical kinetics to the rational design of therapeutic strategies against amyloid aggregation disorders.

1.2. Relevance of Amyloid Fibril Formation to Biomolecular Science

Why is it important to elucidate the molecular mechanisms of amyloid fibril formation? Amyloid fibril formation is believed to be a crucial event in the pathology of a range of devastating and currently incurable medical disorders. There are currently over 50 such conditions that are associated with the amyloid state (16–19), including Alzheimer's disease (associated with the aggregation of the amyloid-β peptide) (20–24), which is currently among the leading causes of death in the Western world (25); Parkinson's disease (α-synuclein) (26); type 2 diabetes (amylin or islet amyloid polypeptide) (27); sickle-cell anemia (haemoglobin) (28); and the prion diseases (prion protein) (29). Thus, it is of key importance to develop effective therapeutic strategies to combat these diseases. As such, there has been longstanding interest in understanding the mechanisms

of pathological amyloid formation. Moreover, elucidating how the formation of these fibrillar protein aggregates can be prevented has become a central focus of current biomedical science and drug discovery (30–32).

Hydrophobic effect: hydrophobic ("water-fearing") forces derive from the thermodynamic driving force to minimize the surface area of nonpolar molecules exposed to an aqueous solvent

Although amyloid fibrils were first discovered in the context of disease, it was later realized that the amyloid state also can be involved in many functional biological processes and can contribute to normal cell and tissue physiology (33). Important examples of functional amyloids include a class of protein hormones that are stored as amyloid-like structures in secretory granules of the endocrine system (34); fungal prions; and the amyloid protein Pmel17, which plays a role in the pigmentation of mammalian skin (35). Functional amyloids, such as the curli fibers on the surface of *Escherichia coli*, are also found in bacteria, where they constitute a major proteinaceous component of bacterial biofilms and hence play important roles in host cell adhesion, invasion, and induction of the host inflammatory response (36–39). Functional amyloids also play other roles, such as protecting the surfaces of certain organisms, including fungi (using hydrophobins) (40), the silkmoth embryo (41), and fish eggs (42), via the hydrophobic effect. Finally, because of their unique materials properties, amyloid fibrils are widely used as biomaterials for nanotechnology (43–50), with various interdisciplinary applications, such as in food science (51).

2. KINETICS OF AMYLOID FIBRIL FORMATION

2.1. Reaction Mechanisms for Amyloid Fibril Formation

What do we mean by elucidating reaction mechanisms for a process like amyloid fibril formation, which involves the constant rearranging of very large numbers of interactions between the species involved? For simple chemical transformations, elucidating the reaction mechanism means breaking down the overall process into a series of elementary molecular events that connect reactants to products (52). Chemical kinetics, and in particular rate laws, which are the workhorse of chemical kinetics, provide the technology for performing this task (see the sidebar titled Chemical Reaction Kinetics). The derivation of integrated rate laws is the foundation for linking the concentrations of reactants and products with the rates of the elementary steps in the underlying reaction mechanism, and hence for testing mechanistic hypotheses through a quantitative comparison between experimental data and model predictions when the reaction conditions are varied. By analogy to the study of simple chemical transformations, the first challenge in the elucidation of a reaction mechanism for amyloid aggregation is to identify the most general set of physically meaningful elementary steps that lead to amyloid fibril formation and to quantify them through a differential rate law that explicitly describes the population balance of each of the aggregate species present during the reaction network, i.e., through a master equation. To find, from this master equation, an integrated rate law that can be compared directly with experiments, we exploit several mathematical approaches that allow explicit solutions to the dynamics to be derived in a convenient manner. Subsequently, the most general combination of possible microscopic mechanisms (there might be a number of alternatives) that is consistent with the available experimental data of amyloid fibril kinetics is identified. Ruling out different possible mechanistic scenarios that are inconsistent with specific features of the experimental data is crucial for constraining the possible underlying mechanism.

2.2. Diversity of Molecular-Level Mechanisms Driving Amyloid Formation

The different elementary molecular-level events that contribute to the overall formation of amyloid aggregates can be broadly divided into two main categories (**Figure 2**): events that lead to

Annu. Rev. Phys. Chem. 2018.69:273-298. Downloaded from www.annualreviews.org
Access provided by Cambridge University on 04/22/18. For personal use only.

CHEMICAL REACTION KINETICS

Chemical reaction kinetics is a general framework for discovering and testing reaction mechanisms using experimental measurements. The canonical workflow of chemical reaction kinetics consists of the following three main steps.

First, a differential rate law corresponding to the hypothesized reaction mechanism is formulated. A differential rate law is a set of coupled differential equations that describe how the rates of formation of the various species involved vary with time. It is obtained from the proposed reaction mechanism by applying the principle of mass action only for elementary reactions. A differential rate law therefore includes rate terms of the form $r = k[\mathrm{A}]^a[\mathrm{B}]^b \ldots$ for each reaction event, where [A], [B], etc. are the concentrations of species A, B, etc.; the exponents a, b, etc. are the associated reaction orders; and k is the rate constant.

Second, an integrated rate law is derived. Differential rate laws are often inconvenient for linking the proposed reaction mechanism to experiments; instead, the differential rate law is integrated to yield an integrated rate law for the (measurable) concentrations of the various species as a function of time.

Third, predictions are tested using integrated rate laws, global curve fitting, and exclusion of reaction mechanisms. Given an experimental methodology for measuring the time-dependent concentrations of reactants or products, the last step in the workflow of chemical kinetics consists of fitting the data to integrated rate laws to test the ability of the proposed mechanisms to describe the data; a proposed reaction mechanism is accepted only if the associated rate law is consistent with all collected experimental data. When investigating the underlying mechanism in a given system, a powerful strategy is to consider the most general set of possible mechanisms and to find specific observables that confirm or contradict predictions for specific mechanisms. This can be achieved by considering easily measurable quantities, such as the reaction half-time (the time it takes for half of the initial concentration of reactant species to be consumed by the reaction). The simplest possible model consistent with all observations should be used.

As an example, the differential rate law of an n-th order reaction, $n\mathrm{A} \rightarrow \mathrm{B}$, is $\mathrm{d}[\mathrm{A}]/\mathrm{d}t = -k[\mathrm{A}]^n$, and the integrated rate law reads $1/[\mathrm{A}]^{n-1} = 1/[\mathrm{A}]_0^{n-1} + (n-1)kt$, where $[\mathrm{A}]_0$ is the initial reactant concentration. Using the integrated rate law, we can make specific predictions about the system that can be tested using experimental data. For example, the reaction half-time is $t_{1/2} = (2^{n-1}-1)/(n-1)k[\mathrm{A}]_0^{n-1}$. Importantly, $t_{1/2}$ obeys a scaling relationship with the initial reactant concentration of the form $t_{1/2} \propto [\mathrm{A}]_0^{\gamma}$, where the scaling exponent $\gamma = -(n-1)$ is linked to the reaction order n of the underlying reaction; hence, a simple measurement of the reaction half-time with varying initial concentrations of reactant in a double-logarithmic plot directly informs one about the order of the underlying reaction, which, in this example, corresponds to the number of interacting species. This simple example illustrates how the scaling exponent γ of the reaction half-time is able to connect simple macroscopic measurements with the microscopic mechanisms of the underlying reaction. This is the power of chemical kinetics for testing mechanistic hypotheses.

Annu. Rev. Phys. Chem. 2018.69:273-298. Downloaded from www.annualreviews.org
Access provided by Cambridge University on 04/22/18. For personal use only.

an increase in aggregate mass and events that modify the total number of aggregates (53). The first category includes growth events, such as fibril elongation and monomer dissociation. Fibril elongation is typically much faster than monomer dissociation (with the exception of the very final stages of aggregation), and for this reason monomer dissociation is often neglected in descriptions of amyloid formation kinetics (54). The second category is responsible for the formation of new aggregates (nuclei). In a system where monomers and aggregates coexist, there are three general and physically meaningful ways of forming new fibrils: (*a*) directly from monomers in solution, (*b*) from fibrils alone, or (*c*) from any combination of monomers and fibrils. An example of scenario *a* is primary (or spontaneous) nucleation. Primary nucleation can be either homogeneous, when

Fibril elongation: addition of individual monomers to fibril ends

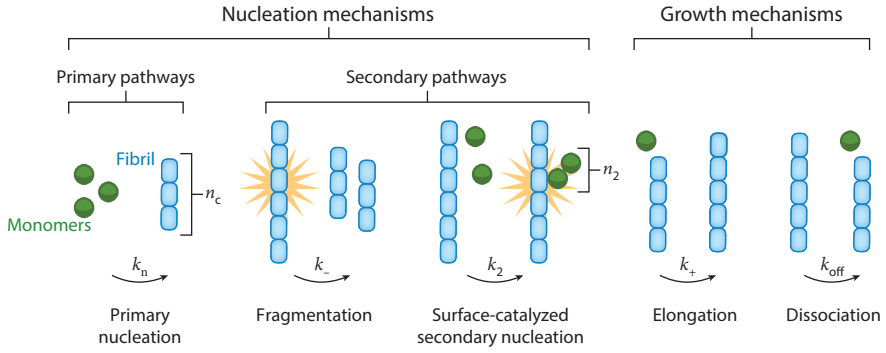

Figure 2

The molecular aggregation mechanisms generating amyloid fibrils can be divided into nucleation (i.e., fibril-forming) and growth mechanisms. Events producing new fibrils are further classified as primary and secondary processes through consideration of whether they depend on the aggregate population. Here, k_n, k_-, k_2, k_+, and k_{off} represent rate constants, and n_c and n_2 represent reaction orders of the primary and secondary pathways.

Annu. Rev. Phys. Chem. 2018.69:273-298. Downloaded from www.annualreviews.org
Access provided by Cambridge University on 04/22/18. For personal use only.

Monomer: elementary assembly building block; monomeric building blocks need not correspond to individual proteins but can include protein complexes (dimers, trimers, etc.)

Monomer dissociation: removal of individual monomers from the ends of fibrils

Nucleus: smallest growth-competent unit of the new structure formed through nucleation

Nucleation: critical step in the formation of a new ordered structure through self-organization; nucleation processes are characterized by the presence of a free energy barrier to form a nucleus

it happens in bulk, or heterogeneous, when it occurs at specific interfaces, such as the air–water interface. An example of heterogeneous primary nucleation is the nucleation of α-synuclein aggregates that has been shown to occur on the surface of lipid vesicles (55). In the absence of preformed fibrillar material, primary nucleation is always the first event in the aggregation reaction. Representative mechanisms for scenarios *b* and *c* are fibril fragmentation and surface-catalyzed secondary nucleation, respectively. Note that secondary nucleation is different from heterogeneous primary nucleation; indeed, while in heterogeneous primary nucleation the formation of new aggregates is facilitated by the presence of any external surface, during secondary nucleation the formation of new aggregates takes place specifically on the surface of existing fibrils, and hence the amount of catalytic surface changes with time in proportion to how many aggregates have been generated. Fibril formation events that depend on the population of existing aggregates are referred to as secondary processes to distinguish them from primary pathways that instead depend solely on the concentration of free monomers. A key characteristic that distinguishes secondary from primary pathways is that secondary mechanisms function as autocatalytic feedback loops: Existing fibrils are effectively able to self-replicate, resulting in an exponential increase of aggregate number and mass concentration. This important feature of secondary processes is experimentally evident in the shape of measured aggregation curves of several proteins, which display long and very flat lag phases followed by a rapid increase typical of exponential growth (see e.g., the experimental data in **Figure 3**).

2.3. Differential Rate Law for Amyloid Fibril Kinetics

The next step in the investigation of the mechanism of amyloid fibril formation is the formulation of a differential rate law for the aggregation kinetics. This goal can be achieved by determining how the concentration $f(t, j)$ of aggregates of size j changes with time t. Accounting for the general classes of elementary mechanisms of amyloid formation discussed in Section 2.2, the time evolution of $f(t, j)$ is described by a nonlinear (mean-field) master equation (see the sidebar titled Master Equation Formalism for Amyloid Fibril Formation), which in the presence of the primary

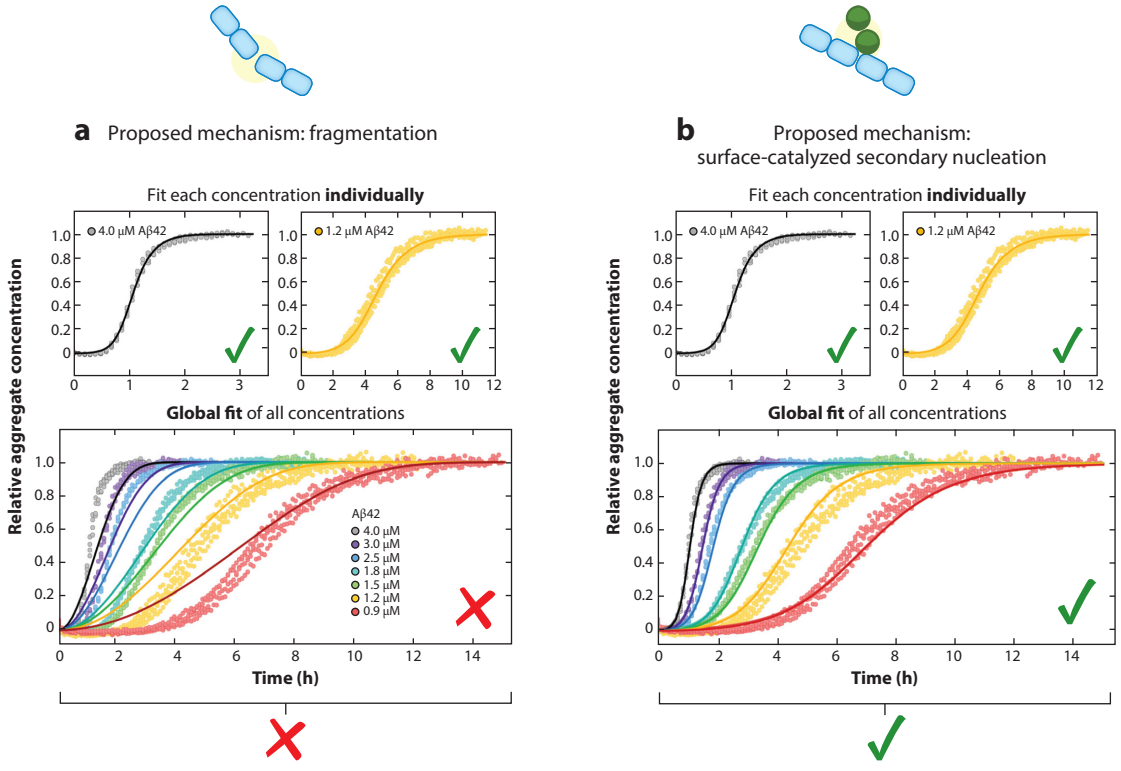

Figure 3

Difference between individual (*top panels*) and global (*bottom panels*) fitting of amyloid-β42 (Aβ42) aggregation kinetics. This example illustrates that fits of individual kinetic traces do not provide sufficient evidence for accepting or rejecting a particular suggested mechanism; mechanistic hypotheses on amyloid fibril aggregation must instead be tested through global fitting over a sufficient range of different protein concentrations. Figure adapted from Reference 56 with permission.

and secondary nucleation pathways takes the form (59, 60)

$$\begin{aligned}\frac{\partial f(t,j)}{\partial t} &= 2k_+ m(t) f(t,j-1) - 2k_+ m(t) f(t,j) \\ &\quad + 2k_- \sum_{i=j+1}^{\infty} f(t,i) - k_-(j-1) f(t,j) \\ &\quad + k_n m(t)^{n_c}\, \delta_{j,n_c} + k_n m(t)^{n_2} \sum_{i=n_c}^{\infty} i f(t,i)\, \delta_{j,n_2}, \\ \frac{\mathrm{d}m(t)}{\mathrm{d}t} &= -\sum_{j=n_c}^{\infty} j \frac{\partial f(t,j)}{\partial t}, \end{aligned} \quad 1.$$

where n_c and n_2 describe the reaction orders of the primary and secondary pathways with respect to the monomer concentration $m(t)$, while k_+, k_-, k_n, and k_2 are the rate constants for fibril elongation, fibril breakage, and primary and secondary nucleation, respectively. The Kronecker delta symbol $\delta_{i,j}$ is equal to one when $i = j$ and zero otherwise. It is important to note that the reaction orders for primary and secondary nucleation, n_c and n_2, do not necessarily correspond to the actual size of the respective nuclei (61, 62) (see Section 3.1). This master equation can be

Primary nucleation: proteins in solution spontaneously come together to form new fibrillar aggregates

Fragmentation: existing aggregates can break at any location along their length, yielding two new aggregates, independently of monomer concentration

Annu. Rev. Phys. Chem. 2018.69:273-298. Downloaded from www.annualreviews.org
Access provided by Cambridge University on 04/22/18. For personal use only.

MASTER EQUATION FORMALISM FOR AMYLOID FIBRIL FORMATION

Master equations are a workhorse of statistical mechanics and describe the time evolution of systems undergoing random transitions between their various states in terms of transition probabilities (57, 58). In the context of amyloid formation, the current state of the system can be described by a vector $\mathbf{N} = (N_1, N_2, \ldots, N_j, \ldots)$, where N_j is the number of filaments with j monomers. As a result of the various microscopic events that drive amyloid formation, the system may probabilistically undergo a transition from some state $\mathbf{N}$ to some other state $\mathbf{N}'$; the master equation describes how the probability $\mathbb{P}(\mathbf{N}, t)$ that the system is in state $\mathbf{N}$ at time t varies with time as a result of these transitions:

$$\frac{\mathrm{d}\mathbb{P}(\mathbf{N}, t)}{\mathrm{d}t} = \sum_{\mathbf{N}'} [A_m(\mathbf{N}' \to \mathbf{N})\, \mathbb{P}(\mathbf{N}', t) - A_m(\mathbf{N} \to \mathbf{N}')\, \mathbb{P}(\mathbf{N}, t)], \qquad 2.$$

where the A_m terms are the transition probabilities. In the mean-field limit (i.e., when statistical mechanical fluctuations are negligible), we introduce the deterministic concentrations (units M = mol/L) of fibrils of size j at time t as $f(t, j) = \langle N_j \rangle / V \mathrm{N_A}$, where V is the system's volume, $\mathrm{N_A}$ is Avogadro's constant, and $\langle \cdot \rangle$ denotes averaging over the probability distribution $\mathbb{P}(\mathbf{N}, t)$. The mean-field concentrations $f(t, j)$ satisfy a deterministic differential equation called the mean-field master equation (Equation 1), which is obtained though averaging of Equation 2 on both sides. Note that while the master equation (Equation 2) is linear in $\mathbb{P}(\mathbf{N}, t)$, Equation 1 is nonlinear; the nonlinearities emerge because the averaged transition rates depend on products of the mean system composition. Note also that, in the protein aggregation literature, the term master equation is used to indicate the mean-field master equation. One should be aware of this convention. The master equation formalism for amyloid aggregation is based on four main assumptions: (*a*) molecular chaos, (*b*) a diluted system, (*c*) spatial homogeneity (this assumption ensures that reaction rates are given by products of concentrations), and (*d*) a large system. Violation of assumption *d* can occur under spatial confinement, such as in the cellular environment or in microfluidics experiments, and leads to the onset of stochastic behavior (see Section 2.7); under these circumstances, the (probabilistic) master equation (Equation 2) instead of the mean-field master equation (Equation 1) must be used to describe the system.

Annu. Rev. Phys. Chem. 2018.69:273-298. Downloaded from www.annualreviews.org
Access provided by Cambridge University on 04/22/18. For personal use only.

interpreted as a population balance equation that describes how the reactive fluxes of all elementary aggregation mechanisms in action jointly change the population of aggregates of size j with time. For example, the first term on the right side of Equation 1 describes the formation of filaments of size j from the elongation of filaments of size $j - 1$, while the second term describes the loss of filaments of size j when they elongate to form filaments of size $j + 1$; there are two ends per aggregate in the case of fibrils, motivating the factor of 2. Similarly, the terms on the second line of Equation 1 describe the reactive flux toward aggregates of size j from fibril fragmentation; the two terms on the third line of Equation 1 describe the formation of new aggregates by primary and secondary nucleation, respectively. Note that the number of surface sites on a fibril is proportional to its mass, leading to a dependence of the secondary nucleation rate on $M(t) = \sum_{j=n_c}^{\infty} jf(t, j)$. Finally, the last line in Equation 1 describes the time evolution of the monomer concentration upon accounting for conservation of total protein mass, which implies $\mathrm{d}m(t)/\mathrm{d}t = -\mathrm{d}M(t)/\mathrm{d}t$. Under certain conditions, however, the monomer concentration can be assumed to be constant, in which case this last equation would not appear; this situation occurs, for instance, when protein synthesis is able to maintain a constant level of monomeric protein throughout the reaction or when, during the early stages of aggregation, the monomer population has not been depleted significantly.

Surface-catalyzed secondary nucleation: existing fibrils catalyze, on their surface, the formation of new aggregates from monomeric protein in solution

Mathematical approaches for describing amyloid fibril formation can be directed either toward solving Equation 1, an approach discussed in References 63–67, or, more conveniently, toward

studying the lowest principal moments of the size distribution, defined as $P(t) = \sum_{j=n_c}^{\infty} f(t,j)$ and $M(t) = \sum_{j=n_c}^{\infty} jf(t,j)$. Key advantages of this second approach are that $P(t)$ and $M(t)$ correspond to the total number and total mass concentrations of aggregates (and hence directly relate to the most common experimental observables) and that $P(t)$ and $M(t)$ satisfy a simpler set of equations, known as moment equations, which are obtained by summation of Equation 1 over j (59, 60):

$$\begin{aligned} \frac{\mathrm{d}P(t)}{\mathrm{d}t} &= k_n m(t)^{n_c} + k_2 m(t)^{n_2} M(t), \\ \frac{\mathrm{d}M(t)}{\mathrm{d}t} &= -\frac{\mathrm{d}m(t)}{\mathrm{d}t} = 2k_+ m(t) P(t). \end{aligned} \qquad 3.$$

The first line of Equation 3 is a statement of the fact that any increase in the number of fibrils in the system is due either to primary nucleation of monomers in solution or to secondary processes, such as breakage of existing aggregates or surface-catalyzed nucleation. These secondary scenarios are captured by a different choice of the reaction order: $n_2 = 0$ for fragmentation and $n_2 \geq 1$ for (surface-catalyzed) secondary nucleation. The second line of Equation 3 states that any increase in aggregate mass or loss of free monomers occurs primarily through the addition of free monomers at the ends of aggregates; indeed, in the second line of Equation 3, nucleation terms have been neglected compared to filament elongation.

Principal moments: the principal moments of the aggregate size distribution $f(t,j)$ are defined as $I_n(t) = \sum_{j=n_c}^{\infty} j^n f(t,j)$; the lowest moments are $P(t) = I_0(t) = \sum_{j=n_c}^{\infty} f(t,j)$ (fibril number concentration) and $M(t) = I_1(t) = \sum_{j=n_c}^{\infty} jf(t,j)$ (fibril mass concentration)

Lag time: time required for the aggregate mass to reach some threshold value; the mass threshold could, e.g., be chosen to be some critical value of the fluorescence intensity if specific amyloid-sensitive dyes are used to detect aggregation

Half-time: time at which 50% of the monomer concentration has been transformed into aggregates

2.4. Integrated Rate Laws for Amyloid Fibril Kinetics

Having defined the differential rate law governing amyloid fibril formation, the next step in the conventional workflow of chemical kinetics is to obtain integrated rate laws that can be directly compared to experimental data. Several mathematical techniques exist that allow approximative closed-form expressions for the integrated rate law to be obtained (see the sidebar titled Integrated Rate Laws for Amyloid Fibril Formation Kinetics). The main advantage of analytical solutions is that the general physical principles that govern the system's dynamics, such as the emergence of scaling laws and the interplay between the various parameters, are clearly evident in such solutions but are more challenging to determine if only numerical integration methods are used. Closed-form analytical expressions for the integrated rate laws therefore offer the most effective way of exploring the predictive power of theory and hence a natural way of identifying the key parameters that underlie the physics of amyloid fibril formation.

Typical reaction time courses described by the integrated rate laws of amyloid formation display a sigmoidal shape characterized by an initial lag time followed by rapid growth. As the reaction reaches completion, the slope of the kinetic curve decreases due to monomer consumption and the curve reaches a plateau. The initial increase and the approach to the plateau can be more or less sharp and can show characteristic symmetries or asymmetries depending on the dominant underlying mechanism of fibril formation (62, 73). Importantly, analytical integrated rate laws allow testable predictions to be made; the most relevant example is the reaction half-time, $t_{1/2}$, which is found to obey a scaling relationship of the form $t_{1/2} \propto m(0)^{\gamma}$, where γ is the scaling exponent (see the sidebar titled Scaling Exponents as a Guide to the Mechanisms of Amyloid Formation) (59, 60, 73, 77). Therefore, as for the simple example of an n-th order reaction discussed above (see the sidebar titled Chemical Reaction Kinetics), the scaling exponent γ of $t_{1/2}$ in amyloid aggregation provides a convenient way of determining the reaction order of the dominant nucleation mechanism.

2.5. Determining the Rates of Amyloid Formation from Experimental Data

A key application of the master equation approach is the determination of the relative contributions of the different microscopic mechanisms of aggregation to the overall reaction from experimental

Annu. Rev. Phys. Chem. 2018.69:273-298. Downloaded from www.annualreviews.org
Access provided by Cambridge University on 04/22/18. For personal use only.

INTEGRATED RATE LAWS FOR AMYLOID FIBRIL FORMATION KINETICS

A mathematical challenge in the study of amyloid formation is the coupled and nonlinear nature of the underlying differential rate laws. Two main mathematical methods, summarized here, have been developed for constructing accurate approximative integrated rate laws (59, 60, 68).

In self-consistent analysis, the moment equation (Equation 3) is formulated as a fixed-point equation $[P(t), M(t)] = \mathcal{A}[P(t), M(t)]$, which is solved iteratively by repeated application of the fixed-point operator $\mathcal{A}$ on an appropriately chosen initial guess $[P_0(t), M_0(t)]$ [the mathematical theory of fixed-point mappings (69) ensures that this sequence of approximations converges to the exact solution in the limit of many iterations]. The explicit form of $\mathcal{A}$ depends on the specific differential equations under investigation; for Equation 3, it is obtained simply through formal integration:

$$\begin{bmatrix} P(t) \\ M(t) \end{bmatrix} = \mathcal{A} \begin{bmatrix} P(t) \\ M(t) \end{bmatrix} = \begin{bmatrix} k_n \int_0^t m(\tau)^{n_c} \mathrm{d}\tau + k_2 \int_0^t m(\tau)^{n_2} M(\tau) \mathrm{d}\tau \\ m(0) - m(0) e^{-2k_+ \int_0^t P(\tau) \mathrm{d}\tau} \end{bmatrix}. \quad 4.$$

A convenient choice for the starting point of the fixed-point iteration is the solution to the linearized moment equations, $\mathrm{d}P_0/\mathrm{d}t = k_n m(0)^{n_c} + k_2 m(0)^{n_2} M_0(t)$ and $\mathrm{d}M_0/\mathrm{d}t = 2k_+ m(0) P_0(t)$, obtained by assuming $m(t) \approx m(0)$, which is $P_0(t) = k_n m(0)^{n_c} \sinh(\kappa t)/\kappa$ and $M_0(t) = \lambda^2[\cosh(\kappa t) - 1]/\kappa^2$, where $\lambda^2 = 2k_+ k_n m(0)^{n_c}$ and $\kappa^2 = 2k_+ k_2 m(0)^{n_2+1}$ (28, 59, 60, 70). Applying Equation 4 to $P_0(t)$ yields a compact formula for $M(t)$ (59, 60):

$$\frac{M(t)}{m(0)} = 1 - \exp\left(-\frac{\lambda^2}{2\kappa^2} e^{\kappa t} - \frac{\lambda^2}{2\kappa^2} e^{-\kappa t} + \frac{\lambda^2}{\kappa^2} \right). \quad 5.$$

This method has been also applied to study filament annealing (71) and copolymerization (72).

In the Hamiltonian approach to fibril formation kinetics, solutions to the kinetic equations are derived by mapping the moment equations to a Hamiltonian system, thus reducing the growth problem to quadrature (73). This method draws on an analogy with classical mechanics by defining momentum and position coordinates as $q = -\log[m(t)/m(0)]$ and $p = 2k_+ P(t)$. In these coordinates, Equation 3 corresponds to Hamilton's equations for the following Hamiltonian:

$$\mathcal{H} = \frac{p^2}{2} + \lambda^2 \frac{e^{-n_c q}}{n_c} + \kappa^2 \frac{e^{-n_2 q}[n_2 q - (n_2 + 1)]}{n_2(n_2 + 1)};$$

in this framework, amyloid aggregation is thus interpreted as a simple transformation of potential energy (monomers) to kinetic energy (aggregates), and classical conservation of energy implies a relationship between total aggregate and monomer mass concentrations. In particular, when secondary nucleation mechanisms dominate, energy conservation leads to a generalized logistic differential equation, with generalized logistic functions as solutions for the aggregate mass concentration (73):

$$\frac{M(t)}{m(0)} = 1 - \left[1 + \frac{\lambda^2}{2\kappa^2 \theta} e^{\kappa t} \right]^{-\theta}, \quad \theta = \sqrt{2/[n_2(n_2 + 1)]}. \quad 6.$$

These results show that buildup of amyloid fibril mass in the presence of secondary nucleation pathways can be thought of as a simple autocatalytic reaction $n_2 m + M \rightarrow 2M$ (74, 75). In the limit $n_2 = 0$, Equation 6 becomes $M(t)/m(0) = 1 - \exp[-(\lambda^2/2\kappa^2) e^{\kappa t}]$, recovering the superexponential behavior predicted by Equation 5.

data, hence completing the workflow of chemical kinetics. This operation is of crucial importance in many contexts, such as the discovery of inhibitors to suppress aggregation, as discussed in Section 5, and has already revealed important insights into the fundamental mechanisms driving amyloid formation by several proteins associated to human disease. A detailed protocol for obtaining suitable data and analyzing the data in a global manner can be found in Reference 56; nontechnical reviews of kinetic analysis of protein aggregation are given in References 4, 62.

Annu. Rev. Phys. Chem. 2018.69:273-298. Downloaded from www.annualreviews.org
Access provided by Cambridge University on 04/22/18. For personal use only.

SCALING EXPONENTS AS A GUIDE TO THE MECHANISMS OF AMYLOID FORMATION

The reaction half-time $t_{1/2}$ is a robust and easily accessible experimental parameter. An analysis of its dependence on the initial free monomer concentration $m(0)$ can yield powerful insights into the underlying mechanism of amyloid formation through the value of the scaling exponent γ, defined by the relationship $t_{1/2} \propto m(0)^{\gamma}$. The scaling exponent is of the form

$$\gamma = -\frac{1}{2}[(\text{reaction order of the dominant nucleation process}) + (\text{reaction order of elongation})]$$

and can, therefore, be used as a guide toward possible mechanisms. Note that γ depends on both the process that dominates the production of fibril mass $M(t)$ (elongation) and the process that dominates the production of new fibril ends $P(t)$ (a primary or secondary nucleation process); as such, it is not meaningful to speak of a single rate-determining step in the context of amyloid self-assembly reactions (76). Experimentally, the value of γ can be obtained as the slope of the reaction half-time plotted against monomer concentration in a double-logarithmic plot. In the simplest case, γ is a constant, but in some cases, curved half-time plots are encountered. Curved half-time plots are indicative of a change in the reaction order of one of the rate-determining steps. A negative curvature emerges from the switch between two mechanisms that compete in parallel, whereas a positive curvature is indicative of a switch of the rate-determining step in a serial or saturating process. Hence, variations of γ with monomer concentration can give insights into the the topology of the reaction network by indicating the presence of saturating or competing processes. All the mechanisms of aggregation considered here (fragmentation, secondary nucleation, and primary nucleation) may compete in parallel, as they all contribute to the increase in $P(t)$. Also, all processes may consist of several microscopic steps in series, and therefore display saturation; to date, however, saturation has only been observed experimentally for elongation and secondary nucleation. The scaling exponents for a number of common mechanisms are summarized in Reference 76.

Annu. Rev. Phys. Chem. 2018.69:273-298. Downloaded from www.annualreviews.org
Access provided by Cambridge University on 04/22/18. For personal use only.

The most common experimental methods for monitoring the kinetics of fibril formation track the increase in total aggregate mass concentration $M(t)$ as a function of time. These methods include recording the fluorescence signal of amyloid-specific dyes, such as thioflavin T (ThT), as well as more direct experimental methods such as nuclear magnetic resonance (NMR) and circular dichroism spectroscopy (78, 79). The first step in the kinetic analysis of fibril mass formation usually involves the selection of a set of suitable mechanisms for global fitting to the experimental data. This can be achieved by determining the scaling exponent of the reaction half-times with respect to the initial monomer concentration, an easily accessible parameter that allows a narrowing down of the number of possible mechanisms (see the sidebar titled Scaling Exponents as a Guide to the Mechanisms of Amyloid Formation). When the scaling analysis is complete, the mechanisms consistent with the obtained scaling exponent are fitted to the experimental data. Although the time dependence of $M(t)$ alone can already give insights into the underlying mechanism, it generally does not represent a robust quantity to reliably determine the mechanisms (**Figure 3**). The solution to this problem of overinterpretation of kinetic data is to vary an additional degree of freedom, for example by considering aggregation kinetics over a range of different protein concentrations simultaneously. By fitting the obtained large datasets in a global manner, sufficient constraints on possible models can be obtained.

Global fit: in a global fit, a set of kinetic curves recorded at varying protein concentrations are fitted simultaneously using the same choice of parameter values in the integrated rate law and using the experimentally determined values for the initial protein concentrations as input data

An example of an application of this approach is the elucidation of the microscopic mechanisms of aggregation of the 42-residue form of the amyloid-β peptide of Alzheimer's disease (**Figure 4**) (53, 80). This strategy revealed in particular that the aggregation of amyloid-β into amyloid

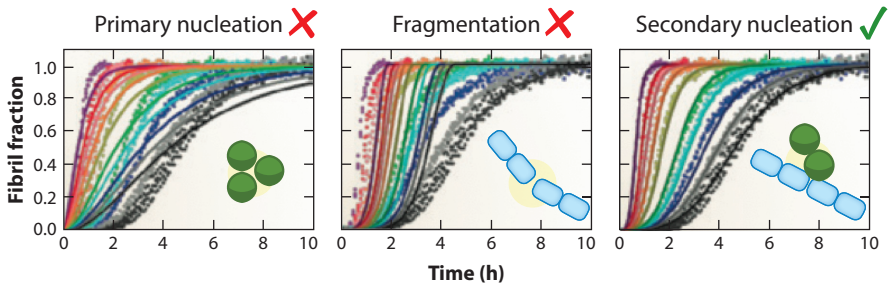

Figure 4

Global best fits of the three models shown schematically to kinetic data of Alzheimer's amyloid-β(1–42) peptide at varying protein concentrations. Both a model lacking any processes of self-replication (primary nucleation) and a model assuming that self-replication occurs via fragmentation fail to reproduce the experimental data. A model assuming that self-replication occurs through surface-catalyzed nucleation of monomers, by contrast, matches the data well at all monomer concentrations, with only three free global fitting parameters in total. Figure adapted from Reference 19.

fibrils is controlled by secondary nucleation processes in the form of aggregate-surface catalysis, a finding that could have important implications in the context of Alzheimer's disease (53, 80, 81). This type of kinetic analysis can be applied more generally to study the dynamical behavior of diverse self-assembling systems ranging from actin to prions and amyloidogenic proteins and is a basis for interpreting and comparing experimental measurements of the formation of filamentous structures in terms of specific mechanisms controlling the proliferation of amyloid fibrils (73).

2.6. Further Methods

For complex aggregation mechanisms, measurements of the total fibril mass concentration $M(t)$ may not be sufficient to thoroughly test the viability of the model and evaluate all parameters of interest. Measurements and analysis of the fibril length distribution, for example obtained by differential sedimentation, may provide the required additional information (66, 67, 82). When the details of the nucleation processes are to be resolved in detail, measurements of the concentration of oligomeric species, e.g., by single-molecule spectroscopy (83), are of interest.

2.7. Spatial Confinement and the Role of Fluctuations

Under spatial confinement, i.e., when the reaction volume approaches scales comparable to the average spatial separation between individual primary nucleation events, the rate of primary nucleation (which depends linearly on reaction volume V) becomes so slow that the aggregation reaction is limited by the waiting time for the first primary nucleation event to occur, causing kinetic traces to be highly variable (84–86). Aggregation then emerges from few, rare nucleation events, which are amplified to detectable concentrations through secondary pathways, typically resulting in Fisher waves (87). An analysis of amyloid aggregation under confinement using (probabilistic) master equations (see the sidebar titled Master Equation Formalism for Amyloid Fibril Formation) (85, 86) predicts that the average lag time, τ_{lag}, satisfies $\langle \tau_{\mathrm{lag}} \rangle = \tau_{\mathrm{bulk}} + c_{\mathrm{n}}/V$, where τ_{bulk} is the deterministic bulk lag time and the parameter $c_{\mathrm{n}}^{-1} = k_{\mathrm{n}} m(0)^{n_c} \mathrm{N_A}$ depends on the rate constant of primary nucleation, k_{n} (84–86). Since τ_{bulk} is independent of V, a plot of $\langle \tau_{\mathrm{lag}} \rangle$ with inverse system volume yields a straight line whose slope provides an estimate for k_{n}. This approach therefore yields important information about the early stages of amyloid formation, which would

Annu. Rev. Phys. Chem. 2018.69:273-298. Downloaded from www.annualreviews.org
Access provided by Cambridge University on 04/22/18. For personal use only.

otherwise be difficult to achieve with experiments in bulk, as these measurements are typically dominated by secondary processes. Moreover, an estimate for the characteristic volume associated with the transition from deterministic bulk kinetics to stochastic behavior is $V_c = \kappa/c_n$; typical values of V_c fall in the range 1 pL–1 nL, which is several orders of magnitude smaller than the typical reaction volumes probed by kinetic experiments in bulk (>1 μL). Droplet microfluidics is particularly suited to this type of study, as it allows the production and monitoring of large numbers of small droplets, a necessary condition to ensure sufficient statistics for readouts of lag times (84). Lag time measurements can be performed in a high-throughput manner using fluorescence microscopy and automated image analysis (84).

3. BRIDGING MICROSCOPIC MECHANISMS AND MACROSCOPIC MEASUREMENTS OF AMYLOID FORMATION USING COARSE-GRAINED COMPUTER SIMULATIONS

Computer simulations can be a powerful tool for exploring the physical driving forces behind a particular phenomenon in isolation from one another, for testing hypotheses that are inaccessible to experiments, and for making experimentally testable predictions. A broad range of computer simulation tools have been developed to describe molecular phenomena across all length and timescales; these methods range from quantum mechanical approaches for probing subatomic behavior to continuum mechanical methods for exploring macroscopic phenomena. Many excellent reviews are dedicated to state-of-the-art computer simulation techniques for investigating amyloid aggregation across scales (88–90). High-resolution models are employed to study the structure and dynamics of single amyloidogenic peptides and proteins and their interactions with a small number of binding partners on short, submicrosecond timescales. The results of such models can be compared with structural methods, such as NMR and X-ray diffraction. However, amyloid formation events, which occur at very low concentrations (nanomolar to micromolar) and on much longer timescales (hours) and length scales (nanometers to micrometers), are inaccessible to such detailed computer simulations. Aggregation on these scales is typically driven by averaged interactions between many molecules and the simultaneous breakage and formation of thousands of weak bonds; hence, not all atomistic details of the aggregating molecules are important. The relevant physics at these scales can be captured by the diffusive motion of macromolecules along energy landscapes determined by the effective intermolecular interactions. This physics can be efficiently captured in coarse-grained computer models, rooted in statistical mechanics and soft matter physics, which retain only crucial ingredients about the shape of molecules and their averaged interactions. The great advantage of these mesoscopic coarse-grained models is that, because of their simplicity, they can capture length and timescales comparable to those probed experimentally. Therefore, the results from coarse-grained simulations can be directly validated against macroscopic experimental measurements. In this sense, coarse-grained computer models offer a unique tool for identifying the set of relevant interactions between individual building blocks that are responsible for the overall kinetic behavior that we have previously described in terms of population balance models. Thus, coarse-grained computer simulations can help us bridge the gap between micro- and macroscales in amyloid formation phenomena.

Here we focus on a particular class of minimalistic coarse-grained models for amyloid aggregation that have proven to be powerful in helping to relate the parameters of kinetic measurements to the underlying physical mechanisms and interactions between individual building blocks that give rise to the overall aggregation behavior (61, 91–97). The first step in designing a model of this class consists of defining the ingredients needed to qualitatively reproduce the available experimental data (see the sidebar titled Coarse-Grained Computer Simulations of Amyloid

Annu. Rev. Phys. Chem. 2018.69:273-298. Downloaded from www.annualreviews.org
Access provided by Cambridge University on 04/22/18. For personal use only.

COARSE-GRAINED COMPUTER SIMULATIONS OF AMYLOID FORMATION

Amyloid fibril formation occurs at length and timescales at which not all molecular details are important; however, since the nuclei are typically smaller than 10 monomers, the continuum limit is not reached either. Coarse-grained simulations are perfectly suited to capturing these intermediate scales, thus providing a bridge between the molecular and macroscopic scales and helping to identify molecular mechanisms behind experimentally measured parameters, such as reaction orders and scaling exponents (**Figure 5*a***). Due to the generality of amyloid behavior, we argue that the underlying physical rules will not depend on the exact details of the proteins involved, so one can employ a generic model to examine the processes behind amyloid formation.

The following minimal ingredients are required to qualitatively reproduce the experimental behavior. (*a*) The protein exists in at least two states: a monomeric and a fibril-forming form. (*b*) The monomeric state can form small disordered oligomers of various sizes, which can be transient, whereas fibrils form irreversibly. (*c*) The conformational change between the monomeric and fibril-forming states is slow and energetically unfavorable, capturing the fact that proteins in the β-sheet–prone state do not usually exist in solution on their own. (*d*) Monomers can adsorb onto fibrils, giving rise to secondary nucleation.

We next describe the coarse-grained model and the choice of parameters. In this model (**Figure 5*b***), the protein is described as a hard rod decorated with a patch that represents generic interactions between monomeric proteins, such as charged, hydrophobic, and polar interactions, as well as hydrogen bonding. These interactions are relatively weak, but still attractive; moreover, they are placed on the tip of the rod, driving the formation of nonstructured oligomers of various sizes. Proteins in the fibril-forming state interact via side-positioned patches, which make particles pack side by side and on top of one another, driving the formation of fibril-like aggregates. The interactions between fibril-forming states are strong so that the irreversibility of amyloid formation can be reproduced. The swap between the monomeric and fibril-forming states is implemented with a small probability and penalized with an excess of chemical potential. To capture secondary nucleation, the patch on the monomeric protein can interact with the fibril surface; the adsorbed monomer can change its conformation into an intermediate, fibril-adsorbed state; the intermediate state interacts more strongly with its own kind than with the fibril state, leading to oligomer detachment. The values of many of the interaction parameters can be estimated from the available experimental and computational data. Although the absolute values of the parameters in such models are not necessarily uniquely defined, their relative ratio needs to be preserved to reproduce the macroscopically observed behavior.

The simulation procedure is as follows. Many ($\sim 10^3$) monomeric proteins are placed inside a large box, giving rise to a particular protein concentration, and evolved using the Monte Carlo (MC) Metropolis scheme. The rates of primary and secondary nucleation are calculated as the inverse of the average lag time (averaged over many repetitions, typically ~10, of the same system with different random seeds); the lag time is the number of MC steps needed for the first nucleus to appear in the simulation. The process is repeated for different initial protein concentrations to obtain the scaling exponents of the primary and secondary nucleation rates with protein concentration.

Annu. Rev. Phys. Chem. 2018.69:273-298. Downloaded from www.annualreviews.org
Access provided by Cambridge University on 04/22/18. For personal use only.

Formation); the model can hence be regarded as a top-down model. Once the model parameters are decided, the simulation framework enables the measurement of the same macroscopic parameters that are accessed in experiments, such as reaction orders and scaling exponents, while retaining information on the underlying molecular mechanisms. In this way, computer simulations can connect molecular mechanisms and macroscopic measurements, explaining the experimentally observed behavior on a molecular level. In addition, such simulations allow us to explore a wide range of parameter space (varying protein concentration, ionic strength, or pH), enabling the testing of possible mechanistic hypotheses. Since virtually any kinetic or thermodynamic quantity can be measured in simulations, this framework uniquely enables us to elucidate the physical

driving forces behind amyloid formation. Below, we provide two examples of how coarse-grained simulations have been used to complement mechanistic analysis based on the master equation formalism in order to bridge the gap between molecular mechanisms and macroscopic experiments in amyloid formation.

Classical nucleation theory (CNT): in CNT, the aggregate size is the only relevant degree of freedom; the free energy profile for the formation of nuclei from a supersaturated solution is a balance between volume free energy, which, in three dimensions, scales as the cube of the aggregate size and describes favorable interactions between monomers, and unfavorable surface free energy, which scales as the square of the aggregate size

3.1. Primary Nucleation of Amyloid Fibrils: Classical or Nonclassical Nucleation?

Primary nucleation of amyloid fibrils involves a marked conformational conversion of the aggregating species accompanied by dynamic changes in the interactions of the aggregating species. These dynamic changes in the nucleating building blocks can give rise to complex phenomena that are not captured by classical nucleation theory (CNT). In particular, an important experimental observation is that the prefibrillar protein oligomers (which are not yet rich in β-sheet content), rather than the mature fibrils, could be the main toxic agents in many amyloid-related diseases (18, 98). It has remained unresolved, however, whether oligomers are necessary for fibril assembly or are just a dangerous byproduct. Computer simulations have shown that, at physiological protein concentrations, amyloid formation must proceed through a two-step process including prefibrillar oligomers (96). Most prevalent oligomers, however, are not of the right size to produce fibrils, and after a long lifetime, they typically dissociate back into solution. Nucleation then proceeds through a preferable oligomer size that is born only in rare fluctuations, which is why such aggregates can be hard to capture experimentally. The free energy profile of this two-step nucleation process via oligomers has been found in computer simulations to have a very different shape from that of the free energy profile typically seen in CNT, such as in the nucleation of crystals (61, 96). This nonclassical character of amyloid nucleation has profound effects on the resulting kinetics. For instance, CNT predicts that the reaction order for fibril nucleation with respect to the free monomer relates to the overall physical size of the nucleating aggregate. Kinetic measurements carried out in computer simulations have revealed that, in two-step amyloid nucleation via oligomers, the reaction order is related to the portion of the aggregate that actively participates in the conformational conversion from the native into the β-sheet–prone state (61). Coarse-grained computer simulations may therefore provide a novel interpretation of the kinetic descriptors of amyloid fibril formation; validation in experiments is currently underway.

3.2. Mechanism of Secondary Nucleation

Coarse-grained computer simulations have also played an important role in identifying the crucial mechanistic steps involved in secondary amyloid nucleation (97). These simulations established that a key physical determinant for this process is the affinity of proteins for the surfaces of fibrils, and that, in order to capture an experimentally observed increase in the rate of secondary nucleation compared to that of primary nucleation, the protein needs to change its conformation when fibril-bound (see the sidebar titled Coarse-Grained Computer Simulations of Amyloid Formation). In this way, the fibril acts as a true catalyst for the formation and detachment of new oligomers from the fibril surface. Strong limits on interprotein interactions were found to be necessary to ensure efficient secondary nucleation; these limits originate from the fact that changes in interprotein interaction strength have opposing effects on the two key steps of secondary nucleation, oligomer formation and oligomer detachment. This narrow region of ideal interprotein interaction values supporting self-replication results in its high specificity and sensitivity to environmental conditions.

A direct practical result from these simulations is the ability to relate the reaction order measured in experiments to the underlying microscopic mechanism. To this end, the simulations were related to experimental kinetic determinants of the self-replication of amyloid-β40 amyloid

Annu. Rev. Phys. Chem. 2018.69:273-298. Downloaded from www.annualreviews.org
Access provided by Cambridge University on 04/22/18. For personal use only.

fibrils (53), one of the two major isoforms of the amyloid-β peptide associated with Alzheimer's disease. It has been experimentally observed that the scaling exponent of the rate of secondary nucleation with respect to monomer concentration is highly dependent on the concentration of the monomeric peptide in solution, suggesting a possible change in the nucleation mechanism over the concentration range (**Figure 5*c***) (53). The same kinetic quantities were then measured in simulations (**Figure 5*c***), where similar trends in the change of the scaling exponent with protein concentration were naturally recovered. Importantly, the simulations were able to identify that the process underlying the switch in kinetic behavior is the saturation of fibril surface coverage, and not a change in mechanism; once the fibril surface is saturated, no further monomers can fit onto it, and the reaction cannot become any faster, no matter how many more monomers are added to the solution (**Figure 5*c***). The simulation data suggest that the rate of self-replication follows the surface saturation as $\ln(\text{rate}) \simeq N^* \ln[Km/(1+Km)]$, where K is the monomer-surface equilibrium binding constant and N^* is a constant related to the size of the nucleating oligomer. After these simulation results, the fibril surface coverage by monomeric peptides was measured in biosensing experiments (**Figure 5*c***), confirming that the change in the reaction order does indeed follow the trend in the change of fibril coverage. Both the simulations and experiments showed that by varying the fibril surface coverage in a controlled manner—e.g., by modulating the interprotein interactions with ionic strength—it is possible to control the kinetics of fibril self-replication. This combination of simulations, theory, and experiments suggests that modulating the adsorption of monomeric proteins onto the surface of protein fibrils may represent a fruitful strategy for limiting the proliferation of protein aggregates in a disease context.

4. THE ROLE OF CHEMICAL KINETICS IN DRUG DISCOVERY

Chemical kinetics in drug discovery is well established as a standard tool in the search for enzyme inhibitors with different mechanisms of action (competitive, noncompetitive, or uncompetitive). It is also used to quantify the potency of these compounds, often achieved by measuring equilibrium dissociation constants, K_D (99). This fundamental approach has been instrumental in the design of drugs, including the discovery of protein kinase inhibitors for the potential treatment of cancer (100).

In the case of inhibiting amyloid formation, a process that is associated with neurodegeneration and over 50 other currently incurable disorders, drug discovery has been very challenging. This difficulty arises in large part from the dynamic nature of the process of amyloid fibril formation and the transient nature of the most toxic forms, which are very challenging to isolate and characterize (101). Moreover, the difficulty of understanding the molecular mechanisms of action of small molecules in interfering with the aggregation process has challenged the discovery of viable therapeutics (102–105). The main approaches in searching for compounds that target the aggregation process of amyloid-forming proteins so far have been aimed at either blocking their production or enhancing the degradation of their aggregated forms (102). More recently, an interesting approach has been employed in which small molecule inhibitors were designed to interfere directly with the aggregation process itself (102, 106). The interest in this approach is attested by the number of small molecules that have reached clinical trials with the aim of directly targeting the aggregation process of amyloid-forming proteins (107–109). Such inhibitors have been designed either against the two structural states of amyloid-forming proteins (the monomeric and fibrillar states) or against the intermediate species (oligomers) that are formed during the aggregation process (110, 111). These approaches have led, however, to unsuccessful clinical trials so far (107). New opportunities have recently emerged from the systematic use of chemical kinetics to study the molecular basis of inhibition of amyloid fibril formation (31). In this section, we

Annu. Rev. Phys. Chem. 2018.69:273-298. Downloaded from www.annualreviews.org
Access provided by Cambridge University on 04/22/18. For personal use only.

Annu. Rev. Phys. Chem. 2018.69:273-298. Downloaded from www.annualreviews.org
Access provided by Cambridge University on 04/22/18. For personal use only.

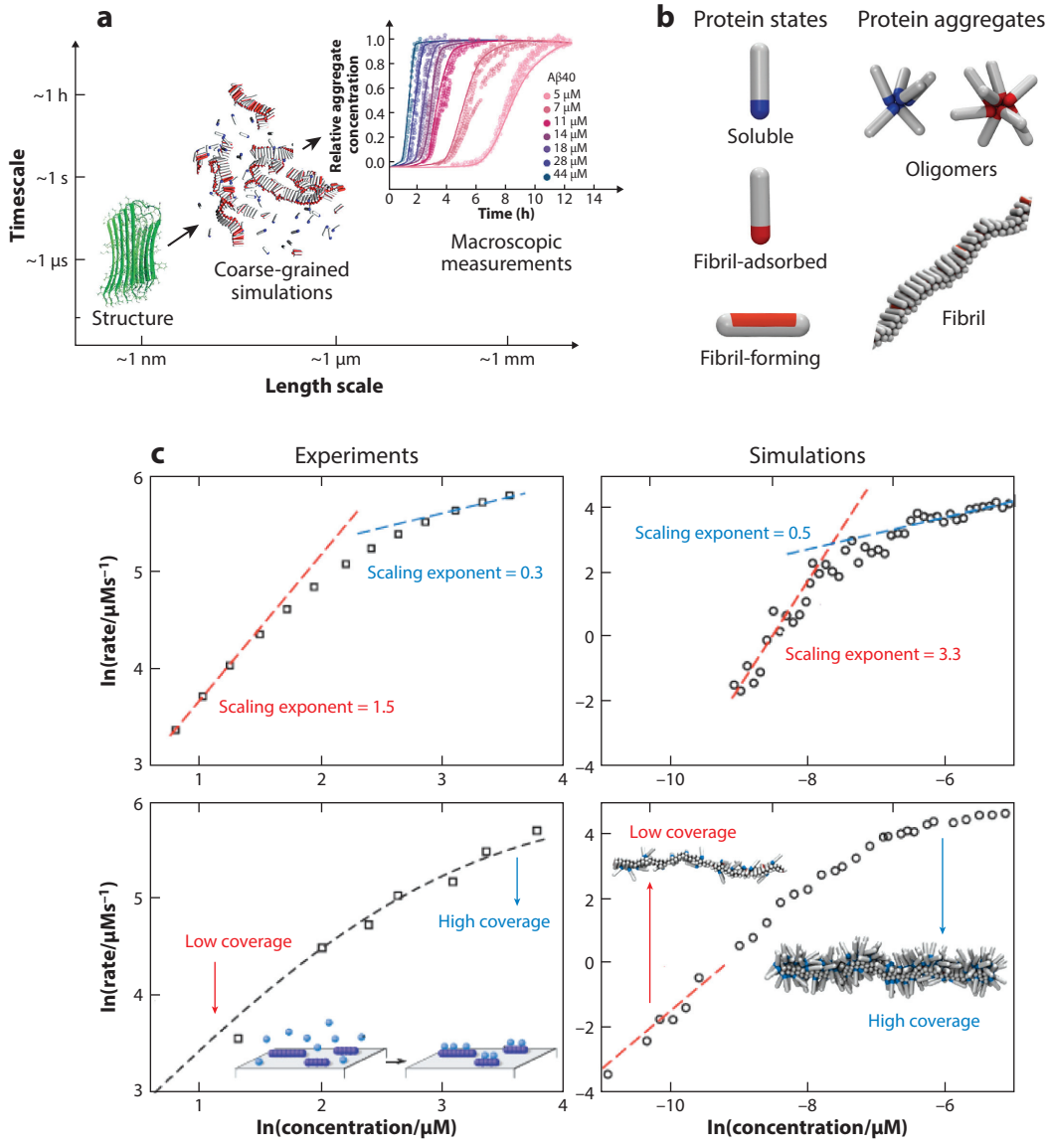

Figure 5

(*a*) Coarse-grained simulations help to connect microscopic and macroscopic scales of amyloid fibril formation. (*b*) Coarse-grained model of amyloid fibril formation (for details, see the sidebar titled Coarse-Grained Computer Simulations of Amyloid Formation). (*c*) Mechanistic understanding of secondary nucleation from coarse-grained simulations. Shown is a comparison of the trends in the scaling kinetic exponents between experiments on the amyloid-β40 (Aβ40) peptide and computer simulations. From the simulations it was predicted that the saturation of the rate is caused by the saturation in the fibril surface coverage, suggesting that the same might be measured in experiments. Independent measurements of the fibril surface coverage have confirmed the predictions from computer simulations, leading to the conclusion that secondary nucleation is driven by the amount of soluble proteins adsorbed onto the fibril surface. Panels *b* and *c* adapted from Reference 97 with permission.

demonstrate how chemical kinetics can help us to understand the mechanism of action of small molecules and to identify and develop potent therapeutic compounds that target specific species in the aggregation process.

4.1. Chemical Kinetics for Identifying the Mode of Action of Inhibitors of Amyloid Fibril Formation

The mechanism of action of a specific inhibitor, as well as its potency in binding to the various species that are present during the aggregation process, can be determined using the master equation framework of chemical kinetics introduced in Section 2. The aggregation process can be inhibited by a small molecule that arrests fibril formation by binding to the monomers, to the mature fibrils, or to low–molecular weight oligomers, which are thought to be primarily responsible for the toxicity associated with protein misfolding diseases (7, 18, 98, 112, 113). Since these possible target species are involved to different orders in each microscopic event that contributes to the formation of fibrils, the final signature of the aggregation profile in the presence of the inhibitors will differ depending on the species to which the inhibitor is bound (**Figure 6**). For example, if a molecule binds to monomers, the differential rate law for monomer concentration becomes

$$\frac{\mathrm{d}m(t)}{\mathrm{d}t} = -2k_+ m(t)P(t) - k_{\mathrm{on}} m(t) C_{\mathrm{i}}(t) + k_{\mathrm{off}} m_{\mathrm{bound}}(t), \qquad 7.$$

where C_{i} is the concentration of inhibitor and k_{on} and k_{off} are the on and off rates for monomer binding (114). The derivation of an integrated rate law for the kinetic equations with binding to monomers (Equation 7) shows that the presence of the inhibition leads to effective reductions in the rate constants (k_n, k_2, k_+) according to the following scheme (114):

$$\frac{k_{\mathrm{n}}^{\mathrm{app}}}{k_{\mathrm{n}}} = \frac{1}{(1 + K_{\mathrm{mon}}^{\mathrm{eq}} C_{\mathrm{i}})^{n_c}}, \quad \frac{k_{+}^{\mathrm{app}}}{k_{+}} = \frac{1}{(1 + K_{\mathrm{mon}}^{\mathrm{eq}} C_{\mathrm{i}})}, \quad \frac{k_{2}^{\mathrm{app}}}{k_{2}} = \frac{1}{(1 + K_{\mathrm{mon}}^{\mathrm{eq}} C_{\mathrm{i}})^{n_2}}, \qquad 8.$$

where $K_{\mathrm{mon}}^{\mathrm{eq}} = k_{\mathrm{on}}/k_{\mathrm{off}}$ is the equilibrium constant for monomer binding. In general, the various mechanisms of inhibition give rise to different, but characteristic, reductions of the rate constants as a function of inhibitor concentration, and the analysis of these characteristic signatures in the overall aggregation profiles represents a useful strategy for elucidating the inhibition mechanism of specific compounds of interest (114). It is therefore possible to determine the species to which the inhibitor is binding by analyzing amyloid aggregation kinetics in the presence of increasing concentrations of the inhibitor.

4.2. Small Molecules Target Amyloid Fibril Formation Through a Variety of Different Mechanisms

The use of chemical kinetics in the study of inhibition of amyloid fibril formation has already allowed the identification of a series of effective compounds to target amyloid fibril formation in different ways. For example, a molecular chaperone, the human Brichos domain, was found to delay amyloid-β42 fibril formation by inhibiting the surface-catalyzed secondary nucleation step by specifically binding to amyloid-β42 fibrils (116). As a consequence, Brichos was found to reduce the population of low–molecular weight oligomeric species formed during the aggregation process, leading to reduced toxicity in mouse brain tissue. This behavior specifically results from the fact that surface-catalyzed secondary nucleation is the main process generating the toxic species.

In another example, the small molecule bexarotene was found to delay amyloid-β42 fibril formation by inhibiting mainly the primary nucleation step (119). From cell experiments, it was shown that targeting the primary nucleation of amyloid-β42 leads to a delay rather than a

Annu. Rev. Phys. Chem. 2018.69:273-298. Downloaded from www.annualreviews.org
Access provided by Cambridge University on 04/22/18. For personal use only.

Annu. Rev. Phys. Chem. 2018.69:273-298. Downloaded from www.annualreviews.org
Access provided by Cambridge University on 04/22/18. For personal use only.

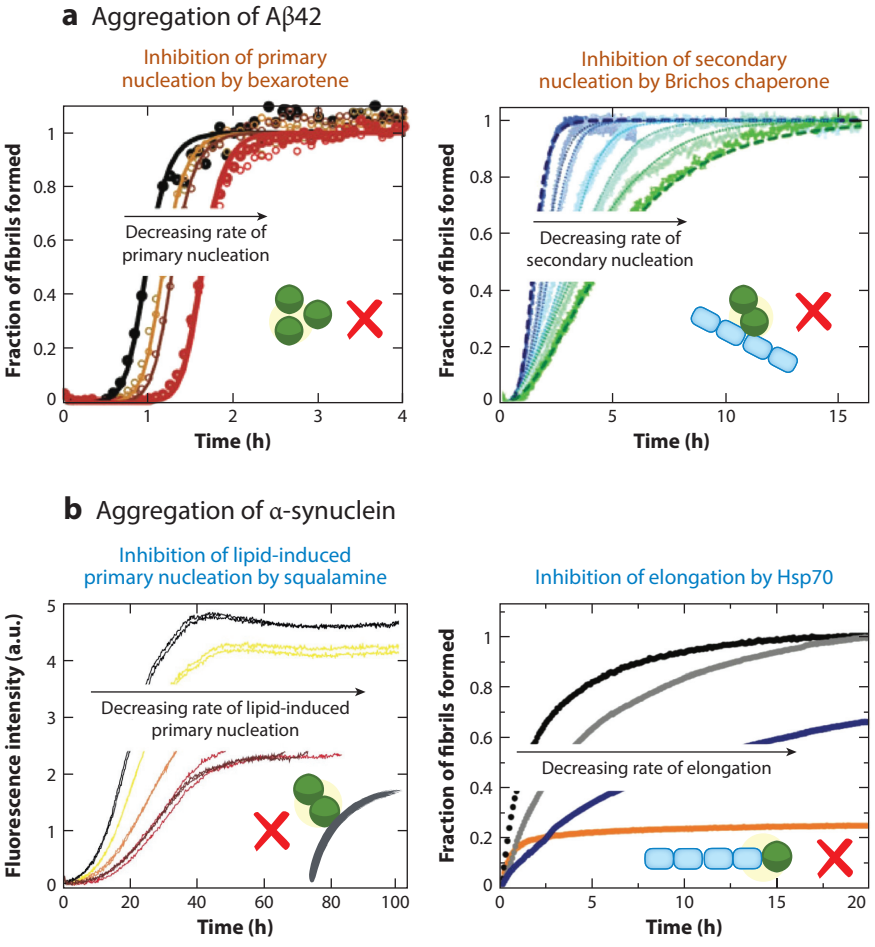

Figure 6

Schematic illustration of the various mechanisms of inhibition in the aggregation of (*a*) amyloid-β42 (Aβ42) and (*b*) α-synuclein. Depending on the species to which the inhibitor is binding, different microscopic processes of the overall aggregation are affected (31, 114). In the aggregation of amyloid-β, molecules may affect the primary nucleation pathway (*a*, *left*), the surface-catalyzed secondary nucleation pathway (*a*, *right*), or the elongation pathway (not shown). In the aggregation of α-synuclein, inhibitors have been reported to interfere with the lipid-induced primary nucleation process (*b*, *left*) or the elongation process (*b*, *right*). Panel *a* adapted from (*left*) Reference 115 and (*right*) Reference 116 with permission. Panel *b* adapted from (*left*) Reference 117 and (*right*) Reference 118 with permission.

reduction of the cytotoxicity associated with the aggregation of amyloid-β42. This was also the case in a *Caenorhabditis elegans* model of amyloid-β42–mediated dysfunction. In this model, an age-progressive paralysis of the worm is observed as the aggregation of amyloid-β42 occurred in body-wall muscle cells. When bexarotene was added at the larval stages, the paralysis induced by the aggregation of amyloid-β42 was delayed to the point of complete recovery. The different biological effects that result from inhibiting different microscopic events clearly exhibit the importance of understanding the mechanism of action of an inhibitor. In the context of disease, this is especially relevant for the timing of drug administration (120). In particular, a preventative

molecule that should be administered as soon as the aggregation process has started, if not before, will not be effective in treating patients with more advanced stages of the disease.

Chemical kinetics–based drug discovery has also been applied to understand the mechanism of action of two small molecules on the aggregation of α-synuclein, where primary nucleation is triggered by the presence of lipid vesicles and secondary nucleation is more favorable under conditions of low pH (55, 121). In this case, squalamine, a natural product, was found to inhibit the initiation of α-synuclein aggregation on the surface of lipid vesicles (117). In a Parkinson's disease model of *C. elegans*, the motility of worms was significantly improved when they were treated with squalamine. By contrast, the 70-kDa heat shock protein Hsp70 was found to bind preferentially to α-synuclein fibrils and to inhibit the elongation process (118).

4.3. Chemical Kinetics: A Unique Opportunity for Drug Discovery Against Amyloid Disorders

Recent work on the inhibition of amyloid fibril formation has highlighted the key role of chemical kinetics in understanding the molecular mechanisms of action of specific drug compounds. The new possibilities offered by chemical kinetics to design small molecules that are able to interfere in a known manner with different species during the amyloid aggregation process are a unique opportunity for drug discovery. For example, traditional drug discovery concepts, such as structure–activity relationships, can be combined with chemical kinetics to systematically identify and then optimize lead compounds against specific microscopic aggregation processes (115). Thus, chemical kinetics is likely to become a vital tool in the development of novel and essential pharmacological approaches toward finding a cure for debilitating protein misfolding diseases.

SUMMARY POINTS

1. Amyloid fibril formation represents an important topic of modern biophysical chemistry research. It is found ubiquitously in biological systems and carries implications for areas ranging from nanotechnology to biomedicine.
2. A large variety of unrelated proteins and peptides have the ability to aggregate into amyloid fibrils, suggesting common underlying physical mechanisms that can be elucidated using physical methods.
3. Application of the general formalism of chemical kinetics to amyloid aggregation provides a strategy for unraveling the intrinsic complexity of amyloid fibril formation and an opportunity to shed light on the molecular-level events that underlie such phenomena from experimental data. Freely available software (**http://www.amylofit.ch.cam.ac.uk**) partially automates this procedure.
4. Studying amyloid aggregation in reaction volumes comparable to cellular volumes provides a useful strategy for zooming in on the early stages of amyloid formation and accurately determining the rate of primary nucleation, which, in systems dominated by secondary pathways, is often poorly constrained by kinetic measurements in bulk.
5. Coarse-grained computer simulations are particularly suited to dealing with the characteristic length and timescales of amyloid fibril formation, allowing one to reproduce many experimental observations, and hence offer great promise for elucidating the mechanisms of amyloid formation in greater detail.

Annu. Rev. Phys. Chem. 2018.69:273-298. Downloaded from www.annualreviews.org
Access provided by Cambridge University on 04/22/18. For personal use only.

6. Chemical kinetics offers an attractive route for designing, in a rational manner, potent drug molecules that can inhibit amyloid formation with a view to suppressing or retarding the pathological effects of protein aggregation.

DISCLOSURE STATEMENT

J.H., M.V., C.M.D., and T.P.J.K. are founders of Wren Therapeutics, a Cambridge University spin-off company active in drug discovery against protein misfolding diseases.

ACKNOWLEDGMENTS

We acknowledge support from the Swiss National Science Foundation (T.C.T.M.); Peterhouse, Cambridge (T.C.T.M.); the Royal Society (A.Š.); the Academy of Medical Sciences (A.Š.); the Wellcome Trust (A.Š., M.V., C.M.D., T.P.J.K.); the Cambridge Centre for Misfolding Diseases (M.V., C.M.D., T.P.J.K.); the Biotechnology and Biological Sciences Research Council (C.M.D., T.P.J.K.); and the Frances and Augustus Newman Foundation (T.P.J.K.). The research leading to these results has received funding from the European Research Council (ERC) under the European Union's Seventh Framework Programme (FP7/2007-2013) through the ERC grant PhysProt (337969).

LITERATURE CITED

1. Dobson CM. 1999. Protein misfolding, evolution and disease. *Trends Biochem. Sci.* 24:329–32
2. Baldwin AJ, Knowles TPJ, Tartaglia GG, Fitzpatrick AW, Devlin GL, et al. 2011. Metastability of native proteins and the phenomenon of amyloid formation. *J. Am. Chem. Soc.* 133:14160–63
3. Fitzpatrick AWP, Debelouchina GT, Bayro MJ, Clare DK, Caporini MA, et al. 2013. Atomic structure and hierarchical assembly of a cross-β amyloid fibril. *PNAS* 110:5468–73
4. Arosio P, Knowles TPJ, Linse S. 2015. On the lag phase in amyloid fibril formation. *Phys. Chem. Chem. Phys.* 17:7606–18
5. Jiménez JL, Nettleton EJ, Bouchard M, Robinson CV, Dobson CM, Saibil HR. 2001. The protofilament structure of insulin amyloid fibrils. *PNAS* 99:9196–201
6. Fändrich M. 2007. On the structural definition of amyloid fibrils and other polypeptide aggregates. *CMLS* 64:2066–78
7. Eisenberg D, Jucker M. 2012. The amyloid state of proteins in human diseases. *Cell* 148:1188–203
8. Lührs T, Ritter C, Adrian M, Riek-Loher D, Bohrmann B, et al. 2005. 3D structure of Alzheimer's amyloid-β (1–42) fibrils. *PNAS* 102:17342–47
9. Sawaya MR, Sambashivan S, Nelson R, Ivanova MI, Sievers SA, et al. 2007. Atomic structures of amyloid cross-β spines reveal varied steric zippers. *Nature* 447:453–57
10. Wasmer C, Lange A, Van Melckebeke H, Siemer AB, Riek R, Meier BH. 2008. Amyloid fibrils of the HET-s(218–289) prion form a β solenoid with a triangular hydrophobic core. *Science* 319:1523–26
11. Jaroniec CP, MacPhee CE, Bajaj VS, McMahon MT, Dobson CM, Griffin RG. 2004. High-resolution molecular structure of a peptide in an amyloid fibril determined by magic angle spinning NMR spectroscopy. *PNAS* 101:711–16
12. Kodali R, Wetzel R. 2007. Polymorphism in the intermediates and products of amyloid assembly. *Curr. Opin. Struct. Biol.* 17:48–57
13. Makin OS, Serpell LC. 2005. Structures for amyloid fibrils. *FEBS J.* 272:5950–61
14. Knowles TPJ, Fitzpatrick AW, Meehan S, Mott HR, Vendruscolo M, et al. 2007. Role of intermolecular forces in defining material properties of protein nanofibrils. *Science* 318:1900–3

Annu. Rev. Phys. Chem. 2018.69:273-298. Downloaded from www.annualreviews.org
Access provided by Cambridge University on 04/22/18. For personal use only.

Annu. Rev. Phys. Chem. 2018.69:273-298. Downloaded from www.annualreviews.org
Access provided by Cambridge University on 04/22/18. For personal use only.

15. Gazit E. 2002. The "correctly folded" state of proteins: is it a metastable state? *Angew. Chem. Int. Ed.* 41:257–59
16. Chiti F, Dobson CM. 2006. Protein misfolding, functional amyloid, and human disease. *Annu. Rev. Biochem.* 75:333–66
17. Chiti F, Dobson CM. 2017. Protein misfolding, functional amyloid, and human disease: a summary of progress over the last decade. *Annu. Rev. Biochem.* 86:27–68
18. Dobson CM. 2017. The amyloid phenomenon and its links with human disease. *Cold Spring Harb. Perspect. Biol.* 9:a023648
19. Knowles TPJ, Vendruscolo M, Dobson CM. 2014. The amyloid state and its association with protein misfolding diseases. *Nat. Rev. Mol. Cell Biol.* 15:384–96
20. Walsh DM, Selkoe DJ. 2007. Aβ oligomers—a decade of discovery. *J. Neurochem.* 101:1172–84
21. Selkoe DJ, Hardy J. 2016. The amyloid hypothesis of Alzheimer's disease at 25 years. *EMBO Mol. Med.* 8:595–608
22. Hardy JA, Higgins GA. 1992. Alzheimer's disease: the amyloid cascade hypothesis. *Science* 256:184–85
23. Selkoe DJ. 2003. Folding proteins in fatal ways. *Nature* 426:900–4
24. Hardy J, Selkoe DJ. 2002. The amyloid hypothesis of Alzheimer's disease: progress and problems on the road to therapeutics. *Science* 297:353–56
25. Alzheimer's Assoc. 2014. Alzheimer's disease facts and figures. *Alzheimer's Dement.* 10:e47–e92
26. Dauer W, Przedborski S. 2003. Parkinson's disease: mechanisms and models. *Neuron* 39:889–909
27. DiFiglia M, Sapp E, Chase KO, Davies SW, Bates GP. 1997. Aggregation of huntingtin in neuronal intranuclear inclusions and dystrophic neurites in brain. *Science* 277:1990–93
28. Ferrone FA, Hofrichter J, Eaton WA. 1985. Kinetics of sickle hemoglobin polymerization. II. A double nucleation mechanism. *J. Mol. Biol.* 183:611–31
29. Rhoades E, Agarwal J, Gafni A. 2000. Aggregation of an amyloidogenic fragment of human islet amyloid polypeptide. *Biochim. Biophys. Acta* 1476:230–38
30. Cohen FE, Kelly JW. 2003. Therapeutic approaches to protein-misfolding diseases. *Nature* 426:905–9
31. Arosio P, Vendruscolo M, Dobson CM, Knowles TPJ. 2014. Chemical kinetics for drug discovery to combat protein aggregation diseases. *Trends Pharmacol. Sci.* 35:127–35
32. Cremades N, Dobson CM. 2017. The contribution of biophysical and structural studies of protein self-assembly to the design of therapeutic strategies for amyloid diseases. *Neurobiol. Dis.* 109(B):178–90
33. Fowler DM, Koulov AV, Balch WE, Kelly JW. 2007. Functional amyloid—from bacteria to humans. *Trends Biochem. Sci.* 32:217–24
34. Maji SK, Perrin MH, Sawaya MR, Jessberger S, Vadodaria K, et al. 2009. Functional amyloids as natural storage of peptide hormones in pituitary secretory granules. *Science* 325:328–32
35. McGlinchey RP, Shewmaker F, McPhie P, Monterroso B, Thurber K, Wickner RB. 2009. The repeat domain of the melanosome fibril protein Pmel17 forms the amyloid core promoting melanin synthesis. *PNAS* 106:13731–36
36. Romero D, Aguilar C, Losick R, Kolter R. 2010. Amyloid fibers provide structural integrity to *Bacillus subtilis* biofilms. *PNAS* 107:2230–34
37. Oh J, Kim JG, Jeon E, Yoo CH, Moon JS, et al. 2007. Amyloidogenesis of type III–dependent harpins from plant pathogenic bacteria. *J. Biol. Chem.* 282:13601–9
38. Collinson SK, Emödy L, Müller KH, Trust TJ, Kay WW. 1991. Purification and characterization of thin, aggregative fimbriae from *Salmonella enteritidis*. *J. Bacteriol.* 173:4773–81
39. Barnhart MM, Chapman MR. 2006. Curli biogenesis and function. *Annu. Rev. Microbiol.* 60:131–47
40. Sunde M, Kwan AH, Templeton MD, Beever RE, MacKay JP. 2008. Structural analysis of hydrophobins. *Micron* 39:773–84
41. Iconomidou VA, Vriend G, Hamodrakas SJ. 2000. Amyloids protect the silkmoth oocyte and embryo. *FEBS Lett.* 479:141–45
42. Podrabsky JE, Carpenter JF, Hand SC. 2001. Survival of water stress in annual fish embryos: dehydration avoidance and egg amyloid fibers. *Am. J. Physiol. Regul. Integr. Comp. Physiol.* 280:R123–31
43. Knowles TPJ, Buehler MJ. 2011. Nanomechanics of functional and pathological amyloid materials. *Nat. Nanotechnol.* 6:469–79

44. Gazit E. 2007. Self-assembled peptide nanostructures: the design of molecular building blocks and their technological utilization. *Chem. Soc. Rev.* 36:1263–69
45. Knowles TPJ, Oppenheim TW, Buell AK, Chirgadze DY, Welland ME. 2010. Nanostructured films from hierarchical self-assembly of amyloidogenic proteins. *Nat. Nanotechnol.* 5:204–7
46. Li C, Adamcik J, Mezzenga R. 2012. Biodegradable nanocomposites of amyloid fibrils and graphene with shape-memory and enzyme-sensing properties. *Nat. Nanotechnol.* 7:421–27
47. Li C, Bolisetty S, Mezzenga R. 2013. Hybrid nanocomposites of gold single-crystal platelets and amyloid fibrils with tunable fluorescence, conductivity, and sensing properties. *Adv. Mater.* 25:3694–700
48. Li C, Alam MM, Bolisetty S, Adamcik J, Mezzenga R. 2011. New biocompatible thermo-reversible hydrogels from PNiPAM-decorated amyloid fibrils. *Chem. Commun.* 47:2913–15
49. Wei G, Su Z, Reynolds NP, Arosio P, Hamley IW, et al. 2017. Self-assembling peptide and protein amyloids: from structure to tailored function in nanotechnology. *Chem. Soc. Rev.* 46:4661–708
50. Ouberai MM, Gomes dos Santos AL, Kinna S, Madalli S, Hornigold DC, et al. 2017. Controlling the bioactivity of a peptide hormone in vivo by reversible self-assembly. *Nat. Commun.* 8:1026
51. Mezzenga R, Fischer P. 2013. The self-assembly, aggregation and phase transitions of food protein systems in one, two and three dimensions. *Rep. Prog. Phys.* 76:046601
52. Müller P. 1994. Glossary of terms used in physical organic chemistry (IUPAC recommendations 1994). *Pure Appl. Chem.* 66:1077–184
53. Meisl G, Yang X, Hellstrand E, Frohm B, Kirkegaard JB, et al. 2014. Differences in nucleation behavior underlie the contrasting aggregation kinetics of the Aβ40 and Aβ42 peptides. *PNAS* 111:9384–89
54. Michaels TCT, Garcia GA, Knowles TPJ. 2014. Asymptotic solutions of the Oosawa model for the length distribution of biofilaments. *J. Chem. Phys.* 140:194906
55. Galvagnion C, Buell AK, Meisl G, Michaels TCT, Vedruscolo M, et al. 2015. Lipid vesicles trigger α-synuclein aggregation by stimulating primary nucleation. *Nat. Chem. Biol.* 11:229–34
56. Meisl G, Kirkegaard JB, Arosio P, Michaels TCT, Vendruscolo M, et al. 2016. Molecular mechanisms of protein aggregation from global fitting of kinetic models. *Nat. Protoc.* 11:252–72
57. Michaels TCT, Knowles TPJ. 2014. Mean-field master equation formalism for biofilament growth. *Am. J. Phys.* 82:476–83
58. Krapivsky PL, Redner S, Ben-Naim E. 2010. *A Kinetic View of Statistical Physics*. Cambridge, UK: Cambridge Univ. Press
59. Knowles TPJ, Waudby CA, Devlin GL, Cohen SIA, Aguzzi A, et al. 2009. An analytical solution to the kinetics of breakable filament assembly. *Science* 326:1533–37
60. Cohen SIA, Vendruscolo M, Welland ME, Dobson CM, Terentjev EM, Knowles TPJ. 2011. Nucleated polymerization with secondary pathways. I. Time evolution of the principal moments. *J. Chem. Phys.* 135:065105
61. Šarić A, Michaels TCT, Zaccone A, Knowles TPJ, Frenkel D. 2016. Kinetics of spontaneous filament nucleation via oligomers: insights from theory and simulations. *J. Chem. Phys.* 145:211926
62. Cohen SIA, Vendruscolo M, Dobson CM, Knowles TPJ. 2012. From macroscopic measurements to microscopic mechanisms of protein aggregation. *J. Mol. Biol.* 421:160–71
63. Cohen SIA, Vendruscolo M, Dobson CM, Knowles TPJ. 2011. Nucleated polymerization with secondary pathways. II. Determination of self-consistent solutions to growth processes described by non-linear master equations. *J. Chem. Phys.* 135:065106
64. Cohen SIA, Vendruscolo M, Dobson CM, Knowles TPJ. 2011. Nucleated polymerization with secondary pathways. III. Equilibrium behavior and oligomer population. *J. Chem. Phys.* 135:065107
65. Michaels TCT, Garcia GA, Knowles TPJ. 2014. Asymptotic solutions of the Oosawa model for the length distribution of biofilaments. *J. Chem. Phys.* 140:194906
66. Michaels TCT, Yde P, Willis JC, Jensen MH, Otzen D, et al. 2015. The length distribution of frangible biofilaments. *J. Chem. Phys.* 143:164901
67. Michaels TCT, Lazell HW, Arosio P, Knowles TPJ. 2015. Dynamics of protein aggregation and oligomer formation governed by secondary nucleation. *J. Chem. Phys.* 143:054901
68. Michaels TCT, Knowles TPJ. 2015. Kinetic theory of protein filament growth: self-consistent methods and perturbative techniques. *Int. J. Mod. Phys. B* 29:1530002

Annu. Rev. Phys. Chem. 2018.69:273-298. Downloaded from www.annualreviews.org
Access provided by Cambridge University on 04/22/18. For personal use only.

69. Khalil HK. 1996. *Nonlinear Systems*. Upper Saddle River, NJ: Prentice-Hall
70. Bishop MF, Ferrone FA. 1984. Kinetics of nucleation-controlled polymerization. A perturbation treatment for use with a secondary pathway. *Biophys. J.* 46:631–44
71. Michaels TCT, Knowles TPJ. 2014. Role of filament annealing in the kinetics and thermodynamics of nucleated polymerization. *J. Chem. Phys.* 140:214904
72. Dear AJ, Michaels TCT, Knowles TPJ. 2016. Dynamics of heteromolecular filament formation. *J. Chem. Phys.* 145:175101
73. Michaels TCT, Cohen SIA, Vendruscolo M, Dobson CM, Knowles TPJ. 2016. Hamiltonian dynamics of protein filament formation. *Phys. Rev. Lett.* 116:038101
74. Morris AM, Watzky MA, Finke RG. 2009. Protein aggregation kinetics, mechanism, and curve-fitting: a review of the literature. *Biochim. Biophys. Acta* 1794:375–97
75. Morris AM, Watzky MA, Agar JN, Finke RG. 2008. Fitting neurological protein aggregation kinetic data via a 2-step, minimal/"Ockham's razor" model: the Finke–Watzky mechanism of nucleation followed by autocatalytic surface growth. *Biochemistry* 47:2413–27
76. Meisl G, Rajah L, Cohen SIA, Pfammater M, Šarić A, et al. 2017. Scaling behaviour and rate-determining steps in filamentous self-assembly. *Chem. Sci.* 8:7087–97
77. Oosawa F, Asakura S. 1975. *Thermodynamics of the Polymerization of Protein*. London: Academic
78. Westermark GT, Johnson KH, Westermark P. 1999. *Amyloid, Prions, and Other Protein Aggregates*. Amsterdam: Elsevier
79. Hellstrand E, Boland B, Walsh DM, Linse S. 2010. Amyloid β-protein aggregation produces highly reproducible kinetic data and occurs by a two-phase process. *ACS Chem. Neurosci.* 1:13–18
80. Cohen SIA, Linse S, Luheshi LM, Hellstrand E, White DA, et al. 2013. Proliferation of amyloid-β42 aggregates occurs through a secondary nucleation mechanism. *PNAS* 110:9758–63
81. Bolognesi B, Cohen SIA, Aran Terol P, Esbjorner EK, Giorgetti S, et al. 2013. Single point mutations induce a switch in the molecular mechanism of the aggregation of the Alzheimer's disease associated Aβ42 peptide. *ACS Chem. Biol.* 9:378–82
82. Gaspar R, Meisl G, Buell A, Young L, Kaminski CF, et al. 2017. Secondary nucleation of monomers on fibril surface dominates α-synuclein aggregation and provides autocatalytic amyloid amplification. *Q. Rev. Biophys.* 50:e6
83. Iljina M, Garcia GA, Dear AJ, Flint J, Narayan P, et al. 2016. Quantitative analysis of co-oligomer formation by amyloid-β peptide isoforms. *Sci. Rep.* 6:28658
84. Knowles TPJ, White DA, Abate AR, Agresti JJ, Cohen SIA, et al. 2011. Observation of spatial propagation of amyloid assembly from single nuclei. *PNAS* 108:14746–51
85. Szavits-Nossan J, Eden K, Morris RJ, MacPhee CE, Evans MR, Allen RJ. 2014. Inherent variability in the kinetics of autocatalytic protein self-assembly. *Phys. Rev. Lett.* 113:098101
86. Michaels TCT, Dear AJ, Kirkegaard JB, Saar KL, Weitz DA, Knowles TPJ. 2016. Fluctuations in the kinetics of linear protein self-assembly. *Phys. Rev. Lett.* 116:258103
87. Cohen SIA, Rajah L, Yoon CH, Buell AK, White DA, et al. 2014. Spatial propagation of protein polymerization. *Phys. Rev. Lett.* 112:098101
88. Morriss-Andrews A, Shea J-E. 2015. Computational studies of protein aggregation: methods and applications. *Annu. Rev. Phys. Chem.* 66:643–66
89. Wu C, Shea J-E. 2011. Coarse-grained models for protein aggregation. *Curr. Opin. Struct. Biol.* 21:209–20
90. Nagel-Steger L, Owen MC, Strodel B. 2016. An account of amyloid oligomers: facts and figures obtained from experiments and simulations. *Chem. Biochem.* 17:657–76
91. Zhang J, Muthukumar M. 2009. Simulations of nucleation and elongation of amyloid fibrils. *J. Chem. Phys.* 130:035102
92. Ruff KM, Khan SJ, Pappu RV. 2014. A coarse-grained model for polyglutamine aggregation modulated by amphipathic flanking sequences. *Biophys. J.* 107:1226–35
93. Ilie IM, den Otter WK, Briels WJ. 2016. A coarse grained protein model with internal degrees of freedom. Application to α-synuclein aggregation. *J. Chem. Phys.* 144:085103

Annu. Rev. Phys. Chem. 2018.69:273-298. Downloaded from www.annualreviews.org
Access provided by Cambridge University on 04/22/18. For personal use only.

94. Bieler NS, Knowles TPJ, Frenkel D, Vácha R. 2012. Connecting macroscopic observables and microscopic assembly events in amyloid formation using coarse grained simulations. *PLOS Comput. Biol.* 8(10):e1002692
95. Vácha R, Linse S, Lund M. 2014. Surface effects on aggregation kinetics of amyloidogenic peptides. *J. Am. Chem. Soc.* 136:11776–82
96. Šarić A, Chebaro YC, Knowles TPJ, Frenkel D. 2014. Crucial role of nonspecific interactions in amyloid nucleation. *PNAS* 111:17869–74
97. Šarić A, Buell AK, Meisl G, Michaels TCT, Dobson CM, et al. 2016. Physical determinants for self-replication of amyloid fibrils. *Nat. Phys.* 12:874–80
98. Ferreira ST, Vieira MNN, De Felice FG. 2007. Soluble protein oligomers as emerging toxins in Alzheimer's and other amyloid diseases. *IUBMB Life* 59:332–45
99. Patrick G. 2009. *An Introduction to Medicinal Chemistry*. Oxford, UK: Oxford Univ. Press
100. Cohen P, Alessi DR. 2013. Kinase drug discovery—what's next in the field? *ACS Chem. Biol.* 8:96–104
101. Necula M, Kayed R, Milton S, Glabe CG. 2007. Small molecule inhibitors of aggregation indicate that amyloid β oligomerization and fibrillization pathways are independent and distinct. *J. Biol. Chem.* 282:10311–24
102. Aguzzi A, O'Connor T. 2010. Protein aggregation diseases: pathogenicity and therapeutic perspectives. *Nat. Rev. Drug Discov.* 9:237–48
103. Cummings J, Zhong K, Bernick C. 2014. The Cleveland Clinic Lou Ruvo Center for Brain Health: keeping memory alive. *J. Alzheimers Dis.* 38:103–9
104. Huang Y, Mucke L. 2012. Alzheimer mechanisms and therapeutic strategies. *Cell* 148:1204–22
105. Becker RE, Greig NH, Giacobini E, Schneider LS, Ferrucci L. 2014. A new roadmap for drug development for Alzheimer's disease. *Nat. Rev. Drug Discov.* 13:156
106. Amijee H, Scopes DI. 2009. The quest for small molecules as amyloid inhibiting therapies for Alzheimer's disease. *J. Alzheimers Dis.* 17:33–47
107. Mangialasche F, Solomon A, Winblad B, Mecocci P, Kivipelto M. 2010. Alzheimer's disease: clinical trials and drug development. *Lancet Neurol.* 9:702–16
108. Bulic B, Pickhardt M, Schmidt B, Mandelkow EM, Waldmann H, Mandelkow E. 2009. Development of tau aggregation inhibitors for Alzheimer's disease. *Angew. Chem. Int. Ed.* 48:1740–52
109. Lashuel HA, Overk CR, Oueslati A, Masliah E. 2013. The many faces of α-synuclein: from structure and toxicity to therapeutic target. *Nat. Rev. Neurosci.* 14:38–48
110. Nie Q, Du XG, Geng MY. 2011. Small molecule inhibitors of amyloid β peptide aggregation as a potential therapeutic strategy for Alzheimer's disease. *Acta Pharmacol. Sin.* 32:545–51
111. Karran E, Hardy J. 2014. A critique of the drug discovery and phase 3 clinical programs targeting the amyloid hypothesis for Alzheimer disease. *Ann. Neurol.* 76:185–205
112. Cremades N, Chen SW, Dobson CM. 2017. Structural characteristics of α-synuclein oligomers. *Int. Rev. Cell Mol. Biol.* 329:79–143
113. Monsellier E, Chiti F. 2007. Prevention of amyloid-like aggregation as a driving force of protein evolution. *EMBO Rep.* 8:737–42
114. Arosio P, Michaels TCT, Linse S, Månsson C, Emanuelsson C, et al. 2016. Kinetic analysis reveals the diversity of microscopic mechanisms through which molecular chaperones suppress amyloid formation. *Nat. Commun.* 7:10948
115. Habchi J, Chia S, Limbocker R, Mannini B, Ahn M, et al. 2016. Systematic development of small molecules to inhibit specific microscopic steps of Aβ42 aggregation in Alzheimer's disease. *PNAS* 114:E200–8
116. Cohen SIA, Arosio P, Presto J, Kurudenkandy FR, Biverstal H, et al. 2015. A molecular chaperone breaks the catalytic cycle that generates toxic Aβ oligomers. *Nat. Struct. Mol. Biol.* 22:207–13
117. Perni M, Galvagnion C, Maltsev A, Meisl G, Müller MBD, et al. 2017. A natural product inhibits the initiation of α-synuclein aggregation and suppresses its toxicity. *PNAS* 114:E1009–17
118. Aprile FA, Arosio P, Fusco G, Chen SW, Kumita JR, et al. 2017. Inhibition of α-synuclein fibril elongation by Hsp70 is governed by a kinetic binding competition between α-synuclein species. *Biochemistry* 56:1177–80

Annu. Rev. Phys. Chem. 2018.69:273-298. Downloaded from www.annualreviews.org
Access provided by Cambridge University on 04/22/18. For personal use only.

119. Habchi J, Arosio P, Perni M, Costa AR, Yagi-Utsumi M, et al. 2016. An anticancer drug suppresses the primary nucleation reaction that initiates the production of the toxic Aβ42 aggregates linked with Alzheimer's disease. *Sci. Adv.* 2:e1501244
120. Golde TE, Schneider LS, Koo EH. 2011. Anti-Aβ therapeutics in Alzheimer's disease: the need for a paradigm shift. *Neuron* 69:203–13
121. Buell AK, Galvagnion C, Gaspar R, Sparr E, Vendruscolo M, et al. 2014. Solution conditions determine the relative importance of nucleation and growth processes in α-synuclein aggregation. *PNAS* 111:7671–76

Annu. Rev. Phys. Chem. 2018.69:273-298. Downloaded from www.annualreviews.org
Access provided by Cambridge University on 04/22/18. For personal use only.

Annual Review of
Physical Chemistry
Volume 69, 2018

Contents

Annu. Rev. Phys. Chem. 2018.69:273-298. Downloaded from www.annualreviews.org
Access provided by Cambridge University on 04/22/18. For personal use only.

Indexes

Errata

An online log of corrections to *Annual Review of Physical Chemistry* articles may be found at http://www.annualreviews.org/errata/physchem

Annu. Rev. Phys. Chem. 2018.69:273-298. Downloaded from www.annualreviews.org
Access provided by Cambridge University on 04/22/18. For personal use only.